

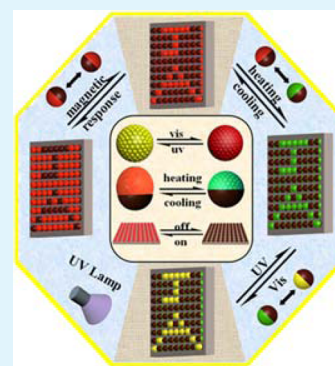
Janus Suprabead Displays Derived from the Modified Photonic Crystals toward Temperature Magnetism and Optics Multiple Responses

Huanhuan Wang, Shengyang Yang,* Su-Na Yin, Li Chen, and Su Chen*

State Key Laboratory of Materials-Oriented Chemical Engineering, College of Chemistry and Chemical Engineering, Nanjing Tech University, No. 5 Xin Mofan Road, Nanjing 210009, P. R. China

ABSTRACT: The design and development of Janus suprabeads (JSs) with multiple responses are highly desirable in the fabrication of functional nanomaterials. In this work, we report a triphase microfluidic strategy for the construction of JSs with temperature-magnetism-optics triple responses. Initially, macromonomer poly(methacrylic acid) (PMAA) obtained via catalytic chain transfer polymerization (CCTP) was grafted onto the polystyrene (PS) colloidal photonic crystals (CPCs) surface. Because abundant carboxylic acid groups in PMAA could coordinate cadmium ions for in situ production of fluorescent CdS quantum dots (QDs) after introducing sulfur ions, the as-prepared JSs were endowed with favorable optical properties. Meanwhile, the as-prepared Cd²⁺/PS CPCs were employed as a template to build JSs with temperature-magnetism sensitivity via the introduction of magnetic Fe₃O₄ and hydrogels. Finally, the fluorescence pattern was easily performed by using chalcogenides as “ink” to write on the pad, in which in situ reaction mechanism was involved in the response. The multiple responsive JSs show promising applications in sensor, display, and anticounterfeit fields.

KEYWORDS: Janus suprabeads, microfluidics, colloidal photonic crystals, sensor, display



INTRODUCTION

The construction of Janus suprabeads (JSs) based on colloidal photonic crystals (CPCs) has received increasing attention because of their versatile applications in remote manipulation,^{1–4} smart nanomaterials (e.g., biological sensors,^{5,6} nanomotors⁷), complex structures, and switchable display devices.^{8–13} To date, a great many routes have been developed to fabricate JSs, including self-assembly, microfluidics, biphasic electrified jetting, protonation–deprotonation cycling, emulsion polymerization, etc.^{14–24} Among them, microfluidic technology as a powerful platform to fabricate JSs with diverse architectures/geometry and versatile functions is vital and efficient because of its simplicity, good repeatability, and high stability.^{25–27} Especially, the construction of CPCs-derived JSs is particular interest due to their unique optical performance. In this respect, Nisisako et al. devised bicolored Janus particles having asymmetric charge distribution and electrical actuation by 2D microfluidic technology for display panel.²⁸ Elaissari group employed miniemulsion polymerization to prepare diverse anisotropic Janus particles with magnetism or fluorescence response.^{15–17} Yang et al. reported the synthesis of Janus balls with electro-responsive photonic performance via optofluidic method, which could be also applied in the display field.²⁹ Previously, our group employed multiple phase microfluidic technology to construct a series of Janus microbeads with dual responses by integrating versatile ionomer-based units, monodisperse CPCs, and functional nanoparticles.^{30–32} However, it is still crucial to simultaneously realize controllable photonic band gaps (PBGs) and multiple

responses (e.g., magnetic, optical, and thermal) in a single unit for environmental monitor or sensor.

Herein, we first time demonstrate an easy-to-perform microfluidic method enabling the assembly of temperature-magnetism-optics triple sensitivity into a single JS. In order to accomplish this triple response JS, we used Cd²⁺-loaded polystyrene (PS) CPCs, *N*-isopropylacrylamide (NIPAm) and Fe₃O₄ nanoparticles as building blocks in the assembly process. Initially, core-shell structured CPCs polystyrene-*co*-poly(methacrylic acid) (PS-PMAA) were obtained from monodispersed PS core and PMAA macromolecules by introducing styrene monomers in the free radical polymerization process. And then, a triphase microfluidic technology was set up to build responsive JSs via coupling magnet and quantum dots (QDs). The successful construction of JSs structures mainly relied on the government of interfacial free energies, which could be realized by optimizing the concentration of surfactants in aqueous solution. Through the magnetic characteristic of JSs, the magneto-responsive switch could be achieved by free-writing on the well-defined panel substrate with a magnetic pen. Besides the magnet response, an on-demand fluorescent pattern was quickly and responsively displayed by a reaction-induced response process. The process was accomplished by the introduction of chalcogenides into JSs, suggesting an alternative way to selectively and effectively assemble QDs-

Received: February 13, 2015

Accepted: April 7, 2015

Published: April 7, 2015

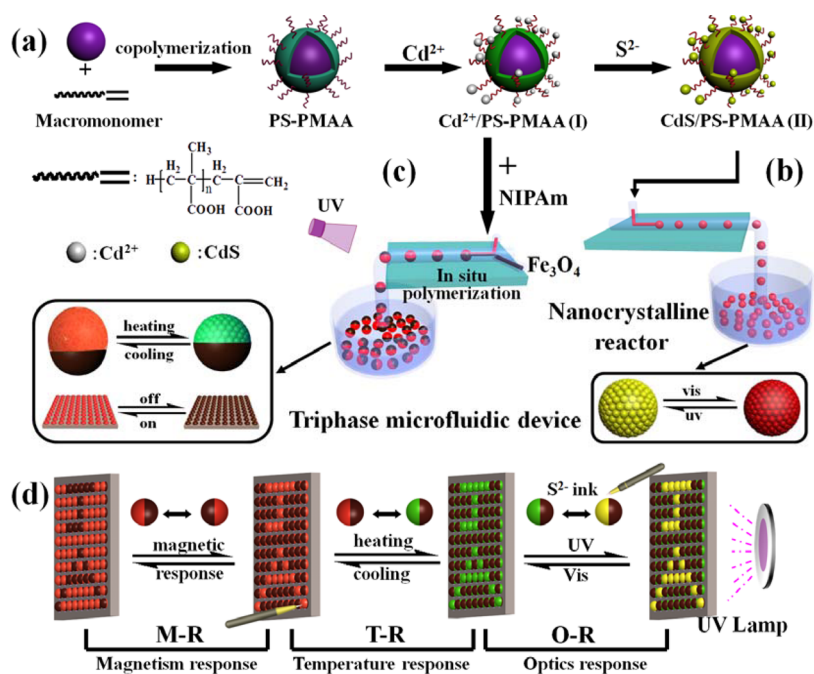


Figure 1. (a) Schematic illustration of the in situ generation of CdS-loaded CPC latex. (b, c) Design of the flow-focusing microfluidic devices to assemble fluorescence suprabeads and temperature-magnetism functional CPC JSs, respectively. (d) The applications of JSs as switches and sensor displays.

integrated CPCs. More importantly, these JSs could be applied to construct multiple functional displays with temperature-magnetism-optics triple sensitivity. The fundamental principle and technological design derived from this study will facilitate the progress in the field of optoelectronic devices and sensors.

EXPERIMENTAL SECTION

Chemicals and Materials. Styrene (St) and methacrylic acid (MAA) were purified with distillation under reduced vacuum to remove impurities. Initiators 2, 2'-azobis [2-(2-imidazolin-2-yl)propane]dihydrochloride (VA-044) was recrystallized in ethanol. Potassium persulfate (KPS), cadmium perchlorate hexahydrate (CdCl₂·6H₂O), sodium sulfide (Na₂S·9H₂O), *n*-hexane, polyvinylpyrrolidone (PVP), *N*-isopropylacrylamide (NIPAm), methylsilicone oil, *N,N'*-methylenebis(acrylamide) (MBA), ethoxylated trimethylolpropane triacrylate (TMPTA, average $M_n = 428$), surfactant (OP-10), Fe₃O₄ (20 nm), and photoinitiator were supplied by Aldrich and used as received. Ultrapure water (18 MΩ cm) from a Milli-Q water system was used throughout the experiments. Bis(aqua)bis((difluoroboryl)dimethylglyoximate)cobalt (CoBF) was employed in the synthesis of PMAA macromonomer according to our previous work.³³

Preparation of PMAA Macromonomer via Catalytic Chain Transfer Polymerization. The PMAA macromonomer was synthesized via catalytic chain transfer polymerization (CCTP) as described previously.³⁴ Briefly, deionized water (150 g), azo-initiator VA-044 (0.3 g), and CoBF (13 mg) dissolved in acetone (2 mL) were added into a 500 mL flask equipped with a magnetic stirrer. For the thorough elimination of oxygen, the flask was consecutively evacuated and purged with high purity nitrogen six freeze-pump-thaw cycles, followed by heating the solution to about 55 °C under continuous stirring. One hour later, an amount of MAA mixed with CoBF (7.5 mg) was added by a syringe. The reaction continued at 55 °C for 1 h and was stopped immediately by ice water. After that, the PMAA macromonomer was isolated by diethyl ether, followed by centrifuging and drying under vacuum.

Synthesis of Monodisperse Functionalized PS-PMAA Microspheres. The synthesis of PS-PMAA microspheres was achieved in this work by emulsion polymerization. First, 5.0 g of St, 0.24 g of PVP, and 100 g of H₂O were added in a 250 mL four-necked

flask equipped with a condenser and continuous stirring. Then, 0.03 g KPS dissolved in 15 g of DI water was slowly added and the reaction was initiated by increasing the temperature to 98 °C. Two hours later, 0.03 g of as-prepared PMAA macromonomers, 0.5 g of St and 5 g of DI water were added dropwise. Finally, the solution of KPS (0.01 g) dissolved in 4.0 g of DI water was added slowly. And, the reaction was terminated after about 1 h. The resulting emulsion was purified with a 200 mesh nylon net to remove minor traces of aggregation.

In Situ Synthesis of CdS QD-Loaded Fluorescent Microspheres. The typical procedure to synthesis of CdS QD-loaded PS-PMAA hybrid latex was carried out as follows. Initially, the as-prepared PS-PMAA was deprotonated in 1 M KOH aqueous solution and the pH of the solution was adjusted to neutral. The excess OH⁻ was removed by centrifugal washing with DI water several times. Next, the latex was treated with 0.1 M CdCl₂·H₂O to conduct ion-exchange between Cd²⁺ and K⁺, followed by the rinse with water to remove excess Cd²⁺. Finally, an amount of 0.1 M Na₂S·9H₂O aqueous solution was added in the purified Cd²⁺-loaded hybrid latex for the reaction (~1 h). The as-obtained fluorescent latex was further purified by centrifugation to remove weakly attached CdS QDs.

Preparation of Fluorescent Suprabeads and Multifunctional JSs by Microfluidic Device. To generate the suprabeads, a microfluidic device was fabricated with a cylindrical polydimethylsiloxane (PDMS) capillary and inner cylindrical 25 G steel needles. Discontinuous and continuous phases were introduced into the needle and the PDMS tube, respectively. For the assembly of fluorescent suprabeads, QDs-loaded CPC latexes were used as the discontinuous phase, while methylsilicone oil was used as the continuous phase and collection phase. The continuous phase broke the inner solutions at the tip of the needle, forming uniform droplets. The fluorescent suprabeads were obtained after solvent evaporation at room temperature (RT) overnight. For the assembly of multifunctional JSs, two discontinuous phases, a solution of Cd²⁺/PS hybrid latex (30 wt %), Am (0.2 wt %), monomers NIPAm (10 wt %), cross-linker MBA (0.02 wt %), surfactant, aqueous photoinitiator 2959 (0.2 wt %), and a mixture of monomers TMPTA, Fe₃O₄ nanoparticles (8 mg/mL), and oil-soluble photoinitiator were introduced into the two needles, respectively. Methylsilicone oil was chosen as the continuous phase. Continuous uniform biphasic droplets formed at the tip of two

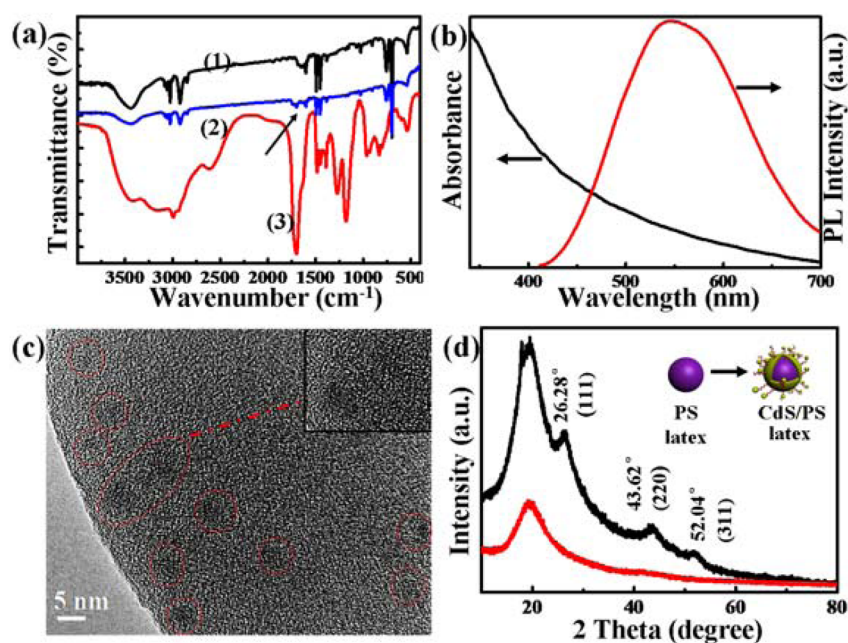


Figure 2. (a) FT-IR spectra of PS microspheres (curve 1), PS-PMAA microspheres (curve 2), and PMAA macromonomers prepared via CCTP (curve 3). (b) UV-vis absorption and PL spectra of CdS/PS-PMAA hybrid latex. (c) TEM images of CdS/PS-PMAA microspheres (the inset is the magnification). (d) XRD spectra of pure PS microspheres (red) and CdS/PS-PMAA hybrid microspheres (black).

needles, followed introducing UV light to photopolymerize.³⁵ The temperature- and magnetic-responsive JSs were finally fabricated.

Characterizations. Fourier transform infrared (FT-IR) spectra were performed on a Nicolet 6700 FT-IR spectrometer to identify the chemical structures of PS-PMAA microspheres. The crystallographic information on the prepared fluorescent CPCs was measured through the power X-ray diffraction (XRD). A Hitachi SEM (scanning electron microscopy) S-4800 was used in a high vacuum mode. A Varian Cary Eclipse spectrophotometer was used in Photoluminescence (PL) measurements. Ultraviolet-visible (UV-vis) absorption spectra were taken with a Perkin-Elmer Lambda 900 UV-vis spectrometer. Transmission electron microscopic (TEM) observation was performed with a JEOL JEM-2010 transmission electron microscope to observe the crystal structure of nanocrystalline on the surface of latex particles. The optical and fluorescence images of the beads were taken using stereoscopic microscope (SMZ800) and confocal microscope, respectively.

RESULTS AND DISCUSSION

To construct temperature-magnetism-optics triple sensitivity CPC JSs, two kinds of building blocks were employed, i.e., monodisperse PS microspheres and Fe_3O_4 nanoparticles. First, uniform PS microspheres were utilized as template for in situ generation of QD-loaded CdS/PS-PMAA hybrid fluorescent microspheres. As shown in Figure 1a, the PMAA macromonomer is first grafted onto the surface of microspheres. It should be noted that the high purity PMAA with terminal double bond groups and abundant carboxylic acid groups was synthesized via CCTP technique.³⁶ The feature of PMAA macromonomer allowed them to graft on the PS surface through the copolymerization with styrene monomers. More importantly, abundant carboxylic acid groups could efficiently capture guest metal ion, achieving a higher concentration of QDs-loaded PS microspheres than traditional method.^{37–39} Indeed, when the PS-PMAA microspheres were immersed into the aqueous solution containing Cd^{2+} , a Cd^{2+} /PS-PMAA microsphere complex was obtained. And then, the as-prepared Cd^{2+} /PS-PMAA further reacted with aqueous chalcogenide

(Na_2S solution) at RT to form a fluorescent CdS/PS-PMAA microsphere (II), which could serve as an independent microreactor.³⁹

On the basis of the above results, we focused on the construction of suprabeads with dual optical performance of structure color and fluorescence in an easy-to-perform microfluidic method (Figure 1b). When these suprabeads were exposed under the light with different wavelengths, they would present varied colors. For instance, they showed red CPC structure color under daylight, whereas they displayed light-yellow fluorescence under ultraviolet light (365 nm). Therefore, the suprabeads with the ability of electronic confinement from the CdS QDs, coupled with photon confinement that arised from the PBGs of the long-range ordered arrays, show great promising applications for optical switching materials.

Moreover, the Cd^{2+} /PS-PMAA complexes were able to be used as building blocks to accomplish temperature-magnetism dual responsive JSs through a triphase microfluidic method. As shown in Figure 1c, the red part represents an aqueous solution containing the Cd^{2+} /PS-PMAA, NIPAm thermal monomer, initiator, and surfactant, while the brown color fluid indicates trimethylolpropane triacrylate (TMPTA) monomer, Fe_3O_4 nanoparticle, and initiator. To achieve Janus morphology by biphasic droplets, the surface tensions of the two parallel phases should be close. However, it is well-known that the surface tension of the aqueous phase is generally much greater than the oil phase. Thus, appropriate amount of surfactant was introduced in the aqueous phase to regulate surface tension, and finally accomplishing JSs structures.^{14,32,40} The solvent evaporation and UV-initiated in situ polymerization afforded JSs droplets with both structure color of CPCs and superparamagnetic properties. Additionally, the filling of the thermosensitive polymer in the CPC structure offered these JSs with controllable PBGs and temperature sensitivity. To the best of our knowledge, this is the first example to assemble temperature-magnetism dual response CPC JSs.

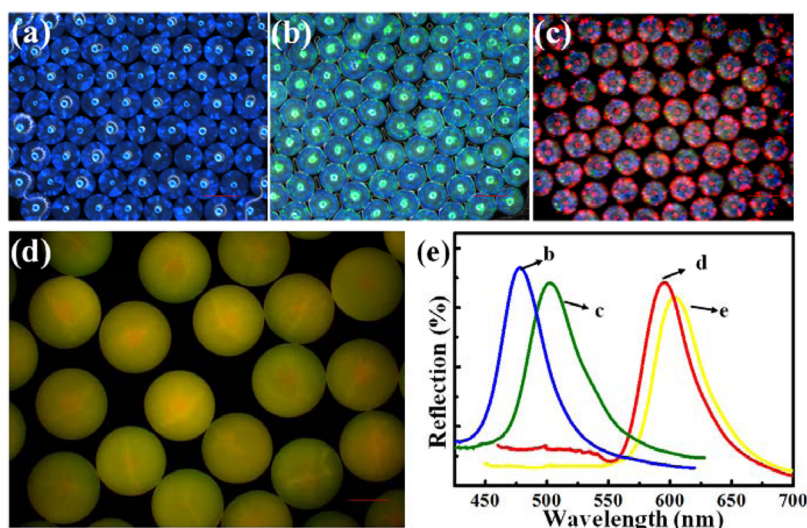


Figure 3. (a–c) Optical micrographs of suprabeads fabricated from PS–PMAA microspheres with different diameter. The scale bars are 350, 380, and 480 μm , respectively. (d) Fluorescent micrograph of CdS hybrid suprabeads (scale bar = 200 μm). (e) Corresponding reflection spectra curves of the suprabead samples shown in a–d.

Interestingly, these temperature-magnetism dual response JSs can act as an independent pixel unit in the multipixel array and easily switch and rotate to realize free-writing on the flat panel by a magnetic pen. As shown in Figure 1d, the letters “JA” are successfully and freely written in the plane substrate. The as-prepared JSs not only show magnetism response when a magnetic pen writes on the panel, but also display reversible temperature response toward color change from red to green when the temperature rises. In addition, after writing with “ink” of chalcogenide ions, the pattern “JA” demonstrates luminescence with bright yellow color under UV light. Notably, although we introduced various components into JSs, their structure color always kept well, facilitating the fabrication of multiple responses for optical switch display under desired conditions.

Figure 2a demonstrates the FT-IR spectra of pure PS microspheres, macromonomer PMAA, and PS–PMAA microspheres. As shown in curve 2, a typical C=O stretching vibration at 1640 cm^{-1} confirms the graft of the macromonomer PMAA onto the surface of PS microspheres, successfully forming PS–PMAA core–shell microspheres.³⁶ After the introduction of sulfur ions at RT, the fluorescent CdS QDs were in situ prepared and encapsulated in PS–PMAA matrix to form hybrid microspheres.^{39,41} Figure 2b shows UV–vis absorption and fluorescent spectra of the resulting CdS/PS–PMAA hybrid latex. A broad photoluminescent emission around 540 nm with the excitation wavelength at 360 nm also indicates the formation of the CdS QDs. Moreover, transmission electron microscopic (TEM) was employed to directly visualize the morphology of CdS QDs. As shown in Figure 2c, well-dispersed CdS QDs without any aggregation are clearly observed due to the advantages of macromonomer PMAA with abundant carboxylic acid groups to stabilize the nanoparticles.³⁶ The structure of CdS QDs was further characterized by XRD. Compared with the diffraction feature of the PS microspheres (Figure 2d), the pattern of CdS hybrid exhibits characteristic peaks at scattering angles of 26.28° , 43.62° , and 52.04° , consistent with scattering from the (111), (220), and (311) planes of a cubic CdS crystal lattice, respectively. The average crystallite

size of CdS QDs is $\sim 3.1\text{ nm}$ calculated via Scherrer equation,⁴² in good agreement with the TEM results.

It is well-known that the structure color of the CPC suprabeads is determined by the size of assembly units. Thus, the different diameter of PS–PMAA colloids will induce variable reflex colors. As shown in Figure 3a–c, the CPC suprabeads present blue, green, and red colors, assembled from PS–PMAA colloids with the diameters of (a) 190, (b) 220, and (c) 280 nm, respectively. It can be clearly found that the ordered and orbicular suprabeads take on unique iridescent surface color. Also, as mentioned above, the suprabeads show yellow fluorescence (Figure 2b) after in situ generation of CdS QDs in polymer matrix. Figure 3d represents the fluorescent image of CdS hybrid suprabeads assembled from the PS–PMAA colloids with particle diameter of 280 nm. Figure 3e reveals the corresponding reflection spectra of CPC suprabeads in Figure 3a–d. When the size of assembly units (i.e., PS–PMAA colloids) increases, the reflex peak shifts to red. However, an abnormal red shift of reflex peak is found in curve d of Figure 3e because the size of assembly units was the same between samples c and d, which could be attributed to the increase in refractive index due to the presence of CdS QDs on the surface of CPCs.³⁹

Subsequently, magnetic thermosensitive multifunctional CPC JSs were accomplished via a triphase microfluidic device (Figures 1c and 4a). After the introduction of Fe_3O_4 nanoparticles (20 nm) and photopolymerization of NIPAm, the as-obtained JSs demonstrate both magnetism and tunable structure color along with temperature variation (Figure 4b). The SEM image of the JS shows a distinct boundary without diffusion around the equator (Figure 4b inset and c). To probe the effect of gels on the morphology of JSs, we further used SEM images to observe the assembly morphology before (Figure 4d) and after (Figure 4e) polymerization of NIPAm. As shown in Figure 4e, the microspheres are filled in the framework of gels, which further suggests the successful polymerization of NIPAm monomers and the complete replacement of the air space by gels in the CPC structure.⁴³ The controlled PBGs and thermosensitivity of the as-prepared JSs are attributed to the hydrogel framework filled in the CPC

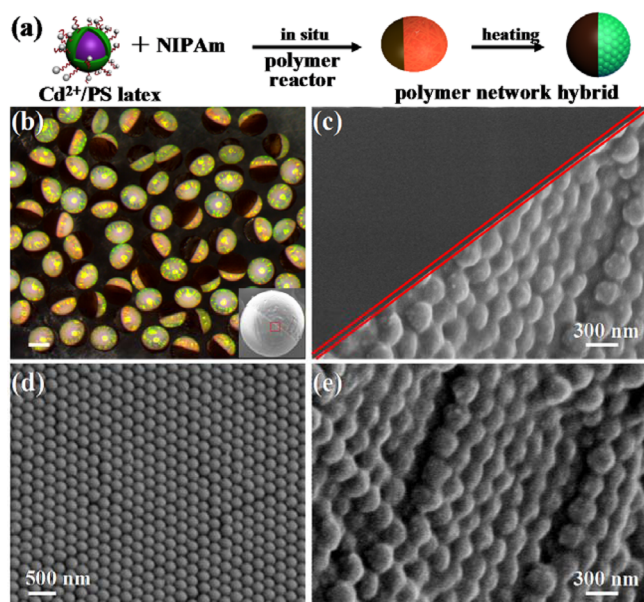


Figure 4. (a) Schematic illustration of the in situ preparation of JSs. (b) Optical micrograph of the bifunctional JSs (scale bar = 400 μm). Inset: a SEM image of a JS. (c) Magnified SEM image of the equator part of a JS. (d, e) SEM photographs of a JS in the CPC part before and after polymerization.

structures. Previously, some thermosensitive suprabeads, such as monodisperse gel-immobilized CPC spheres and double emulsions with colloidal crystal shells have been achieved;^{44,45} however, this work is the first example to construct JSs with the properties that combined structure color, temperature response, and magnetism sensitivity together. Consequently, the as-prepared multifunctional JSs may find diverse applications in environmental sensor.

To investigate the temperature response mechanism for the periodical PBGs change, we observed the suprabeads by optical microscopy under external circulating temperature stimuli. As shown in Figure 5a, when the temperature varies from 46 to 35, 32, and 20 $^{\circ}\text{C}$, the color of the suprabead turns from green to yellow, orange, and red. Because PNIPAm is thermosensitive gel with critical transition temperature of 32 $^{\circ}\text{C}$, when the gels

are immersed into water above this temperature, deswelling immediately occurs at the gel surface. On the contrary, they become hydrophilic below this temperature.^{46–48} Figure 5b shows the reflection spectra of suprabeads exposed at 46, 35, 32, and 20 $^{\circ}\text{C}$. When temperature decreases, the PNIPAm-immobilized CPC suprabead starts to rapidly swell, obviously causing the red shift of PBGs. Notably, both the structure color and reflex spectra are reversible when the temperature decreases again. Figure 5c demonstrates the diameter of the suprabead under different temperature, indicating the decrease in diameter along with the increase in temperature. The PNIPAm gel becomes more hydrophobic and denser under higher temperature, leading to a decrease in water permeability and the size reduction of suprabead.^{44,45} In addition, because the thermosensitive range is close to the body temperature, coupled with the low toxicity and biocompatibility of PNIPAm, the suprabeads show promise for the in vitro medical applications.

In addition, the shift of reflex peak also can be theoretically derived from Bragg diffraction equation

$$\lambda = 2n_c d_{is} \quad (1)$$

where λ is the Bragg wavelength, n_c is the refractive index of the colloidal crystals, and d_{is} is the interplanar spacing of CPC lattice planes. The value of d_{is} is estimated by

$$d_{is} = \left(\frac{2\pi}{9\sqrt{3}} \frac{1}{v_p} \right)^{1/3} d_p \quad (2)$$

where v_p is the particle volume fraction and d_p is the particle diameter. The value of n_c is given by

$$n_c = n_p v_p + n_{pol} v_{pol} + n_w v_w \quad (3)$$

where n is the refractive index, v is the volume fraction, and p , pol , and w indicate nanoparticles, thermosensitive gel, and water, respectively. Because n_p (1.59) > n_{pol} (1.45) > n_w (1.33), the reflex peak shifts to red/blue when the gels absorb/lose water, in agreement with Figure 5b. Thus, CPC suprabeads encapsulated in soft hydrogels with tunable PBGs could quickly distinguish temperature visually compared to traditional gravimetric measurement.^{49,50}

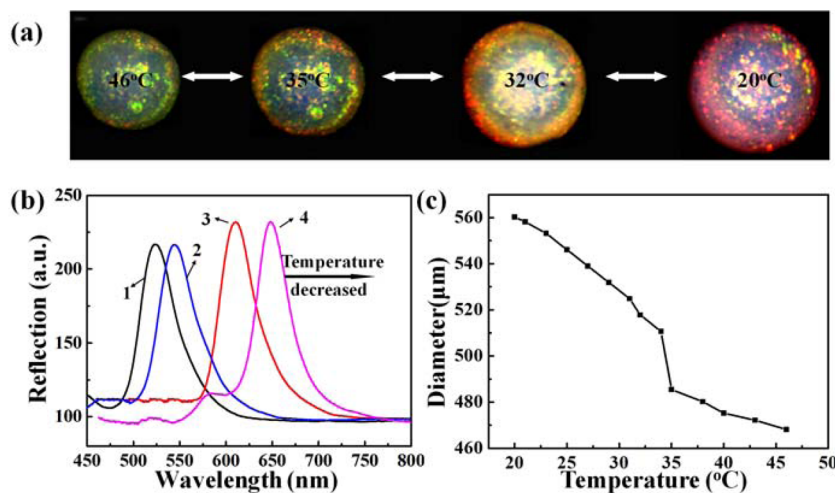


Figure 5. (a) Images of thermosensitive suprabead under varied temperature. (b) Reflectance spectra of the suprabead at 46 (curve 1), 35 (curve 2), 32 (curve 3), and 20 $^{\circ}\text{C}$ (curve 4). (c) The plot of the diameter of the suprabead as a function of temperature.

Finally, we attempted to explore the application of as-prepared JSs for responsive display. Taking the advantage of the magnetic response (M-R), the orientation and motion of JSs could be smoothly switched under variable magnetic fields, allowing them to be pixel units in suprabeads display. For instance, when the rotation axis of the magnet is perpendicular to the substrate, the JSs rotate without any physical translation (Figure 6a).⁴ During the changing cycles of temperature, the

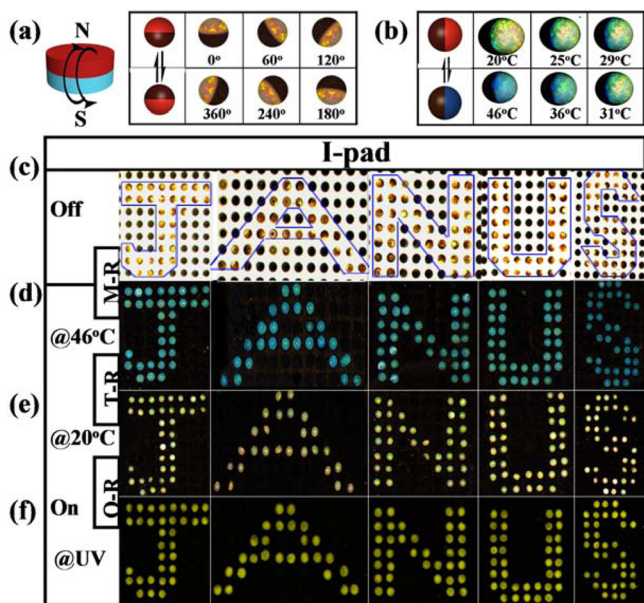


Figure 6. (a) Schematic illustration of the rotational motion of JS under an external magnetic field by a rotating magnet. (b) Reversible color changes of the JS at varied temperature. (c–f) I-pad prepared from multifunctional JSs at (c) “off” state and (d–f) “on” state. (d, e) Optical images of JSs at 46 and 20 °C. (f) Confocal microscopy images of JSs written with chalcogenides.

display color is reversible (Figure 6b). Therefore, the as-obtained pad can simply show images via free-writing based on magnetoresponse, resulting in “off” (Figure 6c) and “on” state (Figure 6d–f). Besides the magnetic response, the pad constructed by JSs can also display based on temperature response (Figure 6d, e), allowing the pad to smartly switch. Another advantage of these JSs is facile access to gain patterns via reaction-induced response. When these JSs are written with chalcogenide, it can be realized the dual optics response (O-R) JSs with both the electronic confinement and photon confinement (Figure 6e, f). These JSs panel displays bright yellow color under UV–vis (Figure 6f), but shows bright CPC structure color (Figure 6e), thereby being potentially useful for anticounterfeit and display with multiple responses.⁵¹

CONCLUSION

In summary, we have in situ fabricated JSs with temperature-magnetism-optics triple sensitivity via an easy-to-perform microfluidic technology. The introduction of thermo-sensitivity monomer and magnetic nanoparticle endows the JSs with various responses to external stimuli. And the JSs can be manipulated to achieve free-writing on the well-defined panel under an external magnetic field. More importantly, taking the unique feature of PMAA macromonomer to coordinate metal ions, we first realized the in situ fabrication of fluorescent CPC suprabeads with high uptake QDs. This process provides a

promising pathway to construct QD-integrated suprabeads and microreactor. To the best of our knowledge, this is the first report to generate the thermosensitivity, fluorescence, and magnetism multiple response Janus sensor displays. We believe this technique can open up ways to design more complex and multifunctional units and offer potential applications in smart display, environmental monitor as well as image codes for anticounterfeiting.

AUTHOR INFORMATION

Corresponding Authors

*E-mail: yangs@njtech.edu.cn . (+86) 25-83172258.

*E-mail: chensu@njtech.edu.cn.

Notes

The authors declare no competing financial interest.

ACKNOWLEDGMENTS

This work was supported by the National High Technology Research and Development Program of China (863 Program) (2012AA030313), National Natural Science Foundation of China (21076103, 21474052 and 21176122), Natural Science Foundation of Jiangsu Province (BK20140934), Priority Academic Program Development of Jiangsu Higher Education Institutions (PAPD), and Qing Lan Project.

REFERENCES

- (1) Chen, C.-H.; Abate, A. R.; Lee, D.; Terentjev, E. M.; Weitz, D. A. Microfluidic Assembly of Magnetic Hydrogel Particles with Uniformly Anisotropic Structure. *Adv. Mater.* **2009**, *21*, 3201–3204.
- (2) Ge, J. P.; Yin, Y. D. Responsive Photonic Crystals. *Angew. Chem., Int. Ed.* **2011**, *50*, 1492–1522.
- (3) Kim, S.-H.; Sim, J. Y.; Lim, J.-M.; Yang, S.-M. Magneto-responsive Microparticles with Nanoscopic Surface Structures for Remote-Controlled Locomotion. *Angew. Chem., Int. Ed.* **2010**, *49*, 3786–3790.
- (4) Rodríguez-López, J.; Shum, H. C.; Elvira, L.; Montero de Espinosa, F.; Weitz, D. A. Fabrication and Manipulation of Polymeric Magnetic Particles with Magnetorheological Fluid. *J. Magn. Magn. Mater.* **2013**, *326*, 220–224.
- (5) Sharma, A. C.; Jana, T.; Kesavamoorthy, R.; Shi, L.; Virji, M. A.; Finegold, D. N.; Asher, S. A. A General Photonic Crystal Sensing Motif: Creatinine in Bodily Fluids. *J. Am. Chem. Soc.* **2004**, *126*, 2971–2977.
- (6) Alexeev, V. L.; Sharma, A. C.; Goponenko, A. V.; Das, S.; Lednev, I. K.; Wilcox, C. S.; David, N. F.; Asher, S. A. High Ionic Strength Glucose-Sensing Photonic Crystal. *Anal. Chem.* **2003**, *75*, 2316–2323.
- (7) Gao, W.; Pei, A.; Dong, R.; Wang, J. Catalytic Iridium-Based Janus Micromotors Powered by Ultralow Levels of Chemical Fuels. *J. Am. Chem. Soc.* **2014**, *136*, 2276–2279.
- (8) Ge, J. P.; Yin, Y. D. Magnetically Tunable Colloidal Photonic Structures in Alkanol Solutions. *Adv. Mater.* **2008**, *20*, 3485–3491.
- (9) Glotzer, S. C.; Solomon, M. J. Anisotropy of Building Blocks and Their Assembly into Complex Structures. *Nat. Mater.* **2007**, *6*, 557–562.
- (10) Lee, S. Y.; Kim, S. H.; Hwang, H.; Sim, J. Y.; Yang, S. M. Controlled Pixelation of Inverse Opaline Structures Towards Reflection-Mode Displays. *Adv. Mater.* **2014**, *26*, 2391–2397.
- (11) Puzzo, D. P.; Arsenault, A. C.; Manners, I.; Ozin, G. A. Electroactive Inverse Opal: A Single Material for All Colors. *Angew. Chem., Int. Ed.* **2009**, *48*, 943–947.
- (12) Wang, X. Q.; Wang, C. F.; Zhou, Z. F.; Chen, S. Robust Mechanochromic Elastic One-Dimensional Photonic Hydrogels for Touch Sensing and Flexible Displays. *Adv. Optical Mater.* **2014**, *2*, 652–662.
- (13) Zhu, C.; Xu, W.; Chen, L.; Zhang, W.; Xu, H.; Gu, Z.-Z. Magneto-chromic Microcapsule Arrays for Displays. *Adv. Funct. Mater.* **2011**, *21*, 2043–2048.

- (14) Kaewsaneha, C.; Tangboriboonrat, P.; Polpanich, D.; Eissa, M.; Elaissari, A. Janus Colloidal Particles: Preparation, Properties, and Biomedical Applications. *Appl. Mater. Interfaces*. **2013**, *5*, 1857–1869.
- (15) Kaewsaneha, C.; Tangboriboonrat, P.; Polpanich, D.; Eissa, M.; Elaissari, A. Facile Method for Preparation of Anisotropic Submicron Magnetic Janus Particles using Miniemulsion. *J. Colloid Interface Sci.* **2013**, *409*, 66–71.
- (16) Kaewsaneha, C.; Bitar, A.; Tangboriboonrat, P.; Polpanich, D.; Elaissari, A. Fluorescent-magnetic Janus Particles Prepared via Seed Emulsion Polymerization. *J. Colloid Interface Sci.* **2014**, *424*, 98–103.
- (17) Kaewsaneha, C.; Tangboriboonrat, P.; Polpanich, D.; Eissa, M.; Elaissari, A. Anisotropic Janus Magnetic Polymeric Nanoparticles Prepared via Miniemulsion Polymerization. *J. Polym. Sci., Part A: Polym. Chem.* **2013**, *51*, 4779–4785.
- (18) Huang, X. P.; Qian, Q. P.; Wang, Y. P. Anisotropic Particles from a One-Pot Double Emulsion Induced by Partial Wetting and Their Triggered Release. *Small* **2014**, *10*, 1412–1420.
- (19) Hwang, S.; Roh, K.-H.; Lim, D. W.; Wang, G. Y.; Uher, C.; Lahann, J. Anisotropic Hybrid Particles Based on Electrohydrodynamic Co-Jetting of Nanoparticle Suspensions. *Phys. Chem. Chem. Phys.* **2010**, *12*, 11894–11899.
- (20) Park, J.; Moon, J.; Shin, H.; Wang, D.; Park, M. Direct-Write Fabrication of Colloidal Photonic Crystal Microarrays by Ink-Jet Printing. *J. Colloid Interface Sci.* **2006**, *298*, 713–719.
- (21) Paunov, V. N.; Cayre, O. J. Supraparticles and “Janus” Particles Fabricated by Replication of Particle Monolayers at Liquid Surfaces Using a Gel Trapping Technique. *Adv. Mater.* **2004**, *16*, 788–791.
- (22) Roh, K.-H.; Martin, D. C.; Lahann, J. Biphasic Janus Particles with Nanoscale Anisotropy. *Nat. Mater.* **2005**, *4*, 759–763.
- (23) Shah, R. K.; Kim, J.-W.; Weitz, D. A. Janus Supraparticles by Induced Phase Separation of Nanoparticles in Droplets. *Adv. Mater.* **2009**, *21*, 1949–1953.
- (24) Smoukov, S. K.; Gangwal, S.; Marquez, M.; Velev, O. D. Reconfigurable Responsive Structures Assembled from Magnetic Janus Particles. *Soft Matter* **2009**, *5*, 1285–1292.
- (25) Hu, Y. D.; Wang, J. Y.; Li, C. N.; Wang, Q.; Wang, H.; Zhu, J. T.; Yang, Y. J. Janus Photonic Crystal Microspheres: Centrifugation-Assisted Generation and Reversible Optical Property. *Langmuir* **2013**, *29*, 15529–15534.
- (26) Yuet, K. P.; Hwang, D. K.; Haghgoeie, R.; Doyle, P. S. Multifunctional Superparamagnetic Janus Particles. *Langmuir* **2010**, *26*, 4281–4287.
- (27) Zhao, Y. J.; Gu, H. C.; Xie, Z. Y.; Shum, H. C.; Wang, B. P.; Gu, Z. Z. Bioinspired Multifunctional Janus Particles for Droplet Manipulation. *J. Am. Chem. Soc.* **2013**, *135*, 54–57.
- (28) Nisisako, T.; Torii, T.; Takahashi, T. T.; Takizawa, Y. Synthesis of Monodisperse Bicolored Janus Particles with Electrical Anisotropy Using a Microfluidic Co-Flow System. *Adv. Mater.* **2006**, *18*, 1152–1156.
- (29) Kim, S.-H.; Jeon, S.-J.; Jeong, W. C.; Park, H. S.; Yang, S.-M. Optofluidic Synthesis of Electroresponsive Photonic Janus Balls with Isotropic Structural Colors. *Adv. Mater.* **2008**, *20*, 4129–4134.
- (30) Liu, S. S.; Wang, C. F.; Wang, X. Q.; Zhang, J.; Tian, Y.; Yin, S. N.; Chen, S. Tunable Janus Colloidal Photonic Crystal Supraballs with Dual Photonic Band Gaps. *J. Mater. Chem. C* **2014**, *2*, 9431–9438.
- (31) Yin, S. N.; Wang, C. F.; Yu, Z. Y.; Wang, J.; Liu, S. S.; Chen, S. Versatile Bifunctional Magnetic-Fluorescent Responsive Janus Supraballs Towards the Flexible Bead Display. *Adv. Mater.* **2011**, *23*, 2915–2919.
- (32) Yu, Z. Y.; Wang, C. F.; Ling, L. T.; Chen, L.; Chen, S. Triphase Microfluidic-Directed Self-Assembly: Anisotropic Colloidal Photonic Crystal Supraparticles and Multicolor Patterns Made Easy. *Angew. Chem., Int. Ed.* **2012**, *51*, 2375–2378.
- (33) Yang, S. Y.; Li, Q.; Chen, L.; Chen, S. Controllable Synthesis of Quantum Dot-Polymer Networks with Enhanced Luminescence via the Catalytic Chain Transfer Polymerization (CCTP) Technique. *J. Mater. Chem.* **2008**, *18*, 5599–5603.
- (34) Chen, L.; Yan, L. L.; Li, Q.; Wang, C. F.; Chen, S. Controllable Synthesis of New Polymerizable Macrosurfactants via CCTP and RAFT Techniques and Investigation of Their Performance in Emulsion Polymerization. *Langmuir* **2010**, *26*, 1724–1733.
- (35) Decker, C. The Use of Irradiation in UV Polymerization. *Polym. Int.* **1998**, *45*, 133–141.
- (36) Yan, L. L.; Yu, Z. Y.; Chen, L.; Wang, C. F.; Chen, S. Controllable Fabrication of Nanocrystal-Loaded Photonic Crystals with a Polymerizable Macromonomer via the CCTP Technique. *Langmuir* **2010**, *26*, 10657–10662.
- (37) Zhang, J.; Coombs, N.; Kumacheva, E.; Lin, Y. K.; Sargent, E. H. A New Approach to Hybrid Polymer-Metal and Polymer-Semiconductor Particles. *Adv. Mater.* **2002**, *14*, 1756–1759.
- (38) Yu, Z. Y.; Wang, C. F.; Chen, S. Fabrication of Quantum Dot-Based Photonic Materials from Small to Large via Inter Facial Self-assembly. *J. Mater. Chem.* **2011**, *21*, 8496–8501.
- (39) Zhang, J.; Ling, L. T.; Wang, C. F.; Chen, S.; Chen, L.; Son, D. Y. Versatile Dendrimer-Derived Nanocrystal Microreactors towards Fluorescence Colloidal Photonic Crystals. *J. Mater. Chem. C* **2014**, *2*, 3610–3616.
- (40) Montagne, F.; Mondain-Monval, O.; Pichot, C.; Elaissari, A. Highly Magnetic Latexes from Submicrometer Oil in Water Ferrofluid Emulsions. *J. Polym. Sci., Part A: Polym. Chem.* **2006**, *44*, 2642–2656.
- (41) Zhang, J. G.; Xu, S. Q.; Kumacheva, E. Polymer Microgels: Reactors for Semiconductor, Metal, and Magnetic Nanoparticles. *J. Am. Chem. Soc.* **2004**, *126*, 7908–7914.
- (42) Klug, H. P.; Alexander, L. E.; *X-Ray Diffraction Procedures: For Polycrystalline and Amorphous Materials*; John Wiley: New York, 1974.
- (43) Yin, S. N.; Wang, C. F.; Liu, S. S.; Chen, S. Facile Fabrication of Tunable Colloidal Photonic Crystal Hydrogel Supraballs toward a Colorimetric Humidity Sensor. *J. Mater. Chem. C* **2013**, *1*, 4685–4690.
- (44) Kanai, T.; Lee, D.; Shum, H. C.; Shah, R. K.; Weitz, D. A. Gel-Immobilized Colloidal Crystal Shell with Enhanced Thermal Sensitivity at Photonic Wavelengths. *Adv. Mater.* **2010**, *22*, 4998–5002.
- (45) Kanai, T.; Lee, D.; Shum, H. C.; Weitz, D. A. Fabrication of Tunable Spherical Colloidal Crystals Immobilized in Soft Hydrogels. *Small* **2010**, *6*, 807–810.
- (46) Heskins, M.; Guillet, J. E. Solution Properties of Poly (N-isopropylacrylamide). *J. Macromol. Sci. Chem.* **1968**, *2*, 1441–1455.
- (47) Zhao, J.; Jiao, K.; Yang, J.; He, C. C.; Wang, H. I. Mechanically Strong and Thermosensitive Macromolecular Microsphere Composite Poly(N-isopropylacrylamide) Hydrogels. *Polymer* **2013**, *54*, 1596–1602.
- (48) Philipp, M.; Aleksandrova, R.; Muller, U.; Ostermeyer, M.; Sanctuary, R.; Muller-Buschbaum, P.; Kruger, J. K. Molecular Versus Macroscopic Perspective on the Demixing Transition of Aqueous PNIPAM Solutions by Studying the Dual Character of the Refractive Index. *Soft Matter* **2014**, *10*, 7297–7305.
- (49) Ashrafal Alam, M.; Takafuji, M.; Ihara, H. Thermosensitive Hybrid Hydrogels with Silica Nanoparticle-cross-linked Polymer Networks. *J. Colloid Interface Sci.* **2013**, *405*, 109–117.
- (50) Lee, W.-F.; Lu, H.-C. Synthesis and Swelling Behavior of Thermosensitive IPN Hydrogels Based on Sodium Acrylate and N-isopropyl Acrylamide by a Two-Step Method. *J. Appl. Polym. Sci.* **2013**, *127*, 3663–3672.
- (51) Lee, H. S.; Shim, T. S.; Hwang, H.; Yang, S.-M.; Kim, S.-H. Colloidal Photonic Crystals toward Structural Color Palettes for Security Materials. *Chem. Mater.* **2013**, *25*, 2684–2690.